Hydrothermal Synthesis and Microstructural, Optical Properties Characterization of YVO_4 Phosphor Powder

S. Zhang[a], Y. Liang[b], X.-Y. Gao[a,*] and H.-T. Liu[a]

[a]Key Laboratory of Materials Physics of Ministry of Education, School of Physics and Engineering Zhengzhou University, 450052 Zhengzhou, China

[b]College of Information Science and Engineering, Henan University of Technology, 450001 Zhengzhou, China

(Received June 13, 2013; in final form November 20, 2013)

The phonon energy of YVO_4 crystal is lower than other usual compounds of salt. So it is suitable as host material for down-conversion materials. Hydrothermal method was adopted to synthesize YVO_4 phosphor powder with the use of yttrium oxide and sodium vanadate as raw material. The change in the relative integral intensity of the (200) and (112) diffraction peaks indicates that macroscopic stress in the lattice obviously changes with the elevated hydrothermal reaction temperature. The YVO_4 phosphor powder synthesized involves a certain agglomeration of small particles. The phonon vibration in the YVO_4 originates mainly from the internal vibrations in the vanadium–oxygen tetrahedron, in addition to the Y–O and O–H vibrations. Due to a low phonon energy of only 2.8188×10^{-21} J, YVO_4 helps to improve the down-conversion efficiency of rare-earth ions. A bandgap value of approximately 3.8 eV for the synthesized YVO_4 powders leads to good absorption properties in the ultraviolet region. Upon excitation by the 320 nm ultraviolet photon, the intrinsic emission of YVO_4 powders is annihilated, and a broadband emission of VO_4^{3-} near 450 nm is observed at room temperature. The YVO_4 phosphor powder synthesized at 180 °C exhibits the maximum photoluminescence intensity because of its excellent crystallization.

DOI: 10.12693/APhysPolA.125.105

PACS 78.55.−m, 42.70.Hj, 78.67.−n

1. Introduction

In the recent years, much research attention has been paid to yttrium vanadate (YVO_4) because of its high chemical and thermal stability as well as low phonon energy. It has been widely used as a matrix material in the field of lighting, optical devices, and diode pumped solid state lasers. For example, YVO_4:Eu^{3+} is a steadfast luminescent material used in color television, the high-pressure mercury lamp and as a scintillator in medical image detectors for more than 20 years [1]. Nd:YVO_4 crystal rather than Nd:YAG has been commercialized as laser device for its excellent monochromaticity and stability [2]. Forbes et al. [3] reported the synthesis, solubility and growth of large YVO_4 and Nd:YVO_4 transparent single crystals in aqueous NaOH under hydrothermal conditions. Moreover, YVO_4 also has certain academic and applied research value as matrix material for down-conversion in crystalline silicon cells. As crystalline silicon cells remain the most dominant solar cell products in the market [4], to achieve large-scale civilian use of crystalline silicon cells, the utilization of solar spectrum, photoelectric conversion efficiency, stability and service life need to be improved. Although photons with energy larger than the silicon band gap can be absorbed, absorption of the ultraviolet photons will increase the internal temperature of the silicon cells. Heat emission inside the cells leads to a decline in cell efficiency, which also affects the stability and service life of battery components. Moreover, the encapsulation glass of battery components can absorb a part of ultraviolet photons, which will reduce the use of ultraviolet photons for solar cells. These phenomena directly limit the further application of crystalline silicon cells [5].

However, a down-conversion mechanism, which is realized by converting a high-energy photon into two or more low-energy photons by using the abundant energy level structure of the rare-earth ions [6], can be used to solve these problems. The down-conversion process is generally realized by doping suitable rare-earth ions into a matrix material with a wide band gap. Efficient energy transfer and conversion between the matrix material and rare-earth ions can be achieved.

For rare-earth ions doped materials, ultraviolet photons with poor response in the solar spectrum can be converted to visible and near-infrared photons that can be easily absorbed by crystalline silicon cells. Through this approach, the loss of ultraviolet photons through encapsulation glass can be reduced and the energy utilization of photons in the ultraviolet region can be enhanced. Thus, the decline in stability of solar cells caused by the direct absorption of ultraviolet photons can be prevented.

A number of studies on single-doped and co-doped rare-earth ions into YVO_4 matrix material have been carried out recently. For example, Ln^{3+} (Ln = Eu, Dy, Sm, and Er) ion-doped YVO_4 nano/microcrystals with multiform morphologies synthesized by hydrothermal method has been reported by Xu et al. [7] in 2010. The spectral conversion for solar cell efficiency enhance-

*corresponding author; e-mail: xygao@zzu.edu.cn

ment using YVO_4:Bi^{3+}, Ln^{3+} (Ln = Dy, Er, Ho, Eu, Sm, and Yb) phosphors synthesized by high-temperature solid phase method has been reported by Huang et al. [8] in 2011. A rapid preparation of YVO_4:Eu^{3+} films by microwave irradiation assisted chemical bath deposition has been reported by Xu et al. [9] in 2005. Of course, the down-conversion phenomena of rare-earth doped materials have also been achieved in various other matrix materials, such as borate [10], phosphate [11] and silicate [12].

Although several methods can be used to synthesize down-conversion materials, a hydrothermal method with the advantages of mild reaction conditions, low cost, simple process, and less vulnerability to pollution compared with the other methods mentioned above has been widely used in the synthesis of rare-earth doped YVO_4 materials. Athough the down-conversion materials of rare-earth doped YVO_4 material has been widely studied, the intrinsic properties of YVO_4, especially the photoluminescence properties and vibration modes of internal chemical bonds, has not been fully understood yet.

In this paper, authors especially focused on the study of the photoluminescence properties and the internal vibration modes of YVO_4 phosphor powder matrix material synthesized by hydrothermal method. The effect of the hydrothermal reaction temperature (HRT) on the microstructure and the optical properties especially photoluminescence property of the phosphor powder were in detail studied on purpose that the study can provide theoretical and experimental basis for further research of rare-earth doped YVO_4 down-conversion luminescent material used in crystal silicon cells.

2. Experimental procedure

A suitable amount of Y_2O_3 (99.99%) was dissolved in hydrochloric acid at an elevated temperature to prepare 0.2 M YCl_3 solution, 20 mL of which was added into a beaker containing 40 mL deionized water. Then, 0.004 mol of Na_3VO_4 (99.99%) was introduced into the solution. After vigorous stirring for 1 h, the as-obtained solution was transferred into a Teflon bottle in a stainless steel autoclave, sealed, and maintained at different HRTs (120, 140, 160, 180, and 200 °C) for 24 h. The autoclave was allowed to cool to room temperature naturally. The precipitates were separated by centrifugation, washed with ethanol and deionized water for several times in sequence, and then dried in air at 80 °C for 12 h. Subsequently, the YVO_4 phosphor powder matrix materials of the HRT series were obtained.

The crystallization, vibration modes, and surface morphology of the YVO_4 phosphor powders were determined through X-ray diffraction (XRD, Philips PANA-lytical X'pert), cold-field scanning electron microscopy (CF--SEM, JEOL-JSM-6700F), Raman spectroscopy (Renishaw 2000), and Fourier transform infrared spectroscopy (FTIR, Nicolet NEXUS-470), respectively. The Scherrer formula was used to calculate the average grain size and lattice microscopic distortion of the phosphor powder. Absorption and luminescence properties were measured through a spectrophotometer (ShimadzuUV-3150) and a spectrofluorometer (FluoroMax-4), respectively. All measurements were carried out at room temperature.

3. Results and discussion

3.1. Crystallization, vibration modes, and surface morphology

Figure 1 shows the XRD patterns of the YVO_4 phosphor powders synthesized by using the hydrothermal method at different HRTs. The products synthesized at different HRTs exhibit the tetragonal and polycrystalline structure of the YVO_4 phase in accordance with the standard diffraction pattern (JCPDS 17-0341). No miscellaneous peak is observed among all the diffraction peaks, indicating that the products are of high purity. The relative integral intensity of the (200) and (112) diffraction peaks gradually decreases with the increase in HRT, with the value abnormally reaching its maximum at 180 °C. This phenomenon indicates that macroscopic stress in the lattice changes with the elevated HRT.

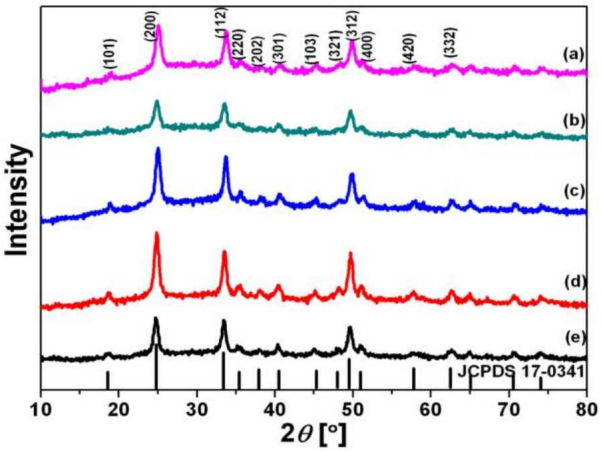

Fig. 1. XRD patterns of the YVO_4 phosphor powders synthesized using the hydrothermal method at HRTs of (*a*) 120 °C, (*b*) 140 °C, (*c*) 160 °C, (*d*) 180 °C, (*e*) 200 °C.

Grain refinement and lattice microscopic distortion lead to XRD-peak broadening. Thus, the full width at half maximum (FWHM) of the XRD diffraction peak of the samples must be corrected when using XRD to characterize the grain size and lattice strain with FWHM can be expressed in accordance with the Williamson–Hall relationship [13, 14]:

$$\beta \cos\theta = \lambda/D + 4\Delta d/d \sin\theta, \tag{1}$$

$$\beta^2 = \beta_M^2 - \beta_S^2, \tag{2}$$

where β is the FWHM of the diffraction peak caused by the grain refinement and lattice microscopic distortion. λ is the wavelength of the X-ray, θ is the Bragg angle, D is the average grain size, d is the spacing between crystal planes, and $\Delta d/d$ is the lattice microscopic distortion.

β_M and β_S are measured FWHM value of the sample and FWHM of standard sample, respectively.

The average grain size and lattice microscopic distortion of the YVO_4 phosphor powders synthesized under different HRTs are shown in Table I. The average grain size of the YVO_4 phosphor powder slightly changes by almost 13 nm as the HRT increases. Moreover, a smaller average grain size results in a larger lattice strain, which is due to the enhanced surface effect [15].

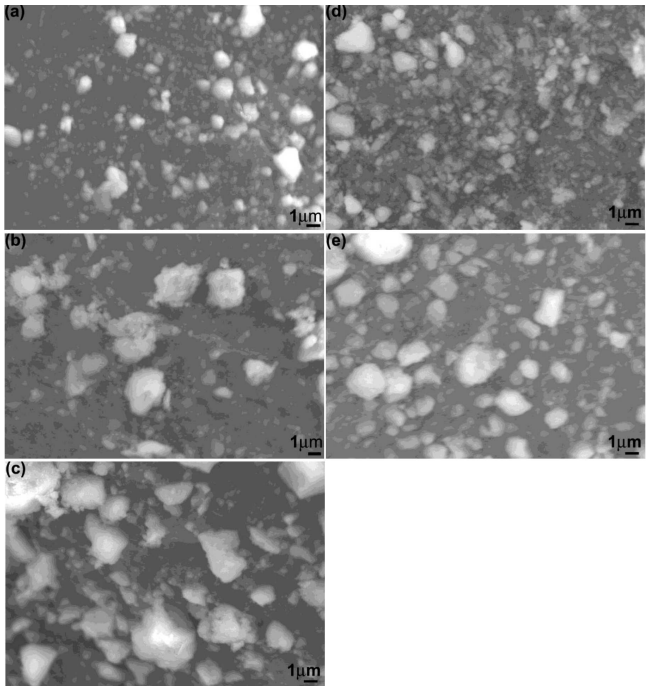

Fig. 2. SEM images of the YVO_4 phosphor powders synthesized at HRTs of (a) 120 °C, (b) 140 °C, (c) 160 °C, (d) 180 °C, (e) 200 °C.

TABLE I

Average grain size and lattice microscopic distortion of the YVO_4 phosphor powders.

HRT [°C]	D [nm]	$\Delta d/d$ [%]
120	12.2	1.499
140	15.8	1.198
160	12.2	1.499
180	12.3	1.408
200	13.8	1.362

Figure 2 presents the SEM images of the YVO_4 phosphor powders synthesized at different HRTs. The phosphor powder synthesized by the hydrothermal method reveals a certain agglomeration of small particles. The particle size is approximately in the micrometer scale. Thus, information on the size and shape of monodispersed particle cannot be obtained from the diagram. These phenomena are related to the randomness of crystal growth along each orientation during the hydrothermal reaction process. This is consistent with the XRD patterns shown in Fig. 1.

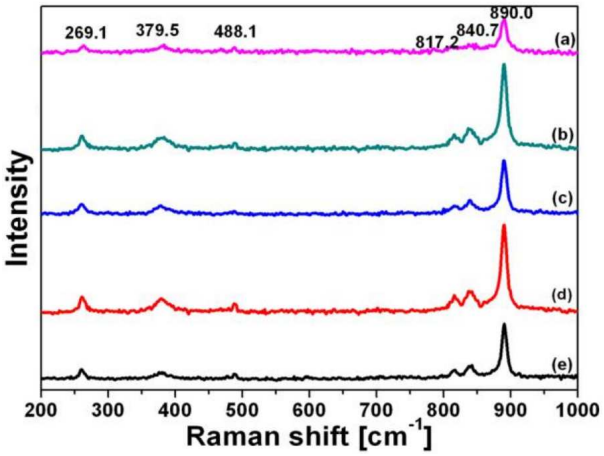

Fig. 3. Raman spectra of the YVO_4 phosphor powders synthesized at HRTs of (*a*) 120 °C, (*b*) 140 °C, (*c*) 160 °C, (*d*) 180 °C, (*e*) 200 °C.

Figure 3 shows the Raman spectra of the YVO_4 phosphor powder synthesized at different HRTs. YVO_4, a uniaxial crystal belonging to the tetragonal zircon-type structure, is assigned to the space group of D_{4h}^{19} and the point group of D_{4h}. The crystal has four kinds of Raman-active vibration modes, including A_{1g}, B_{1g}, B_{2g}, and E_g. The six Raman shift peaks of this crystal are located at 261.9, 379.5, 488.1, 817.2, 840.7, and 890.0 cm^{-1} (Fig. 3), which is consistent with the literature [16, 17]. The six peaks originate from the internal vibrations of the vanadium–oxygen tetrahedron. The vibration symmetry and vibration modes of the Raman shift peaks of YVO_4 crystal synthesized under our experimental conditions were listed in Table II.

TABLE II

Vibration symmetry and vibration modes of the Raman shift peaks of YVO_4 phosphor powder.

Raman shift [cm^{-1}]	Symmetry	Vibration modes
261.9	B_{1g}	symmetrically stretching vibration in VO_4^{3-}
379.5	A_{1g}	symmetrically deformation vibration in VO_4^{3-}
488.1	B_{1g}	antisymmetrically stretching vibration in VO_4^{3-}
817.2	B_{1g}	symmetrically stretching vibration in VO_4^{3-}
840.7	E_g	antisymmetrically deformation vibration in VO_4^{3-}
890.0	A_{1g}	symmetrically stretching vibration in VO_4^{3-}

Table III demonstrates the maximum phonon energy of various common down-conversion matrix materials.

TABLE III

Maximum phonon energy of various common down-conversion matrix materials.

Matrix material	Phonon energy [10^{-21} J]
borate	4.4341
phosphate	3.4839
silicate	3.1672–3.4839
germanate	2.5338–3.0880
yttrium vanadate	2.8188
tellurate	1.9003–2.6921

The Raman spectra (Fig. 3) and Table II show that the phonon energy of YVO_4 is only 2.8188×10^{-21} J (converted from the maximum phonon energy in the Raman spectroscopy), which is lower than other usual compounds of salt. The YVO_4 matrix material with lower phonon energy will generate less heat when joining in the down-conversion process, which is helpful in improving the down-conversion efficiency of rare earth ions-doped YVO_4 phosphor powder. Thus, YVO_4 is suitable as a down-conversion matrix material.

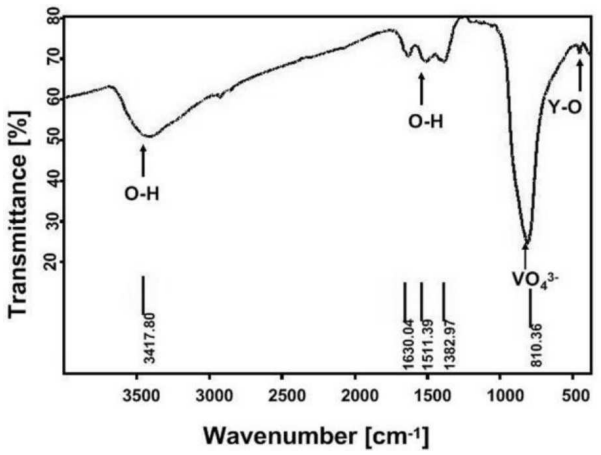

Fig. 4. FTIR spectrum of the YVO_4 phosphor powder synthesized at 180 °C.

Figure 4 presents the FTIR spectrum of the YVO_4 phosphor powder synthesized at 180 °C. The characteristic 810.36 cm^{-1} absorption peak corresponds to the strong VO_4^{3-} absorption band in the region of 780 cm^{-1} to 920 cm^{-1} [18]. Combined with the Raman spectrum, the absorption band may be caused by the superposition of the three characteristic peaks at 817.2, 840.7, and 890.0 cm^{-1}. The 810.36 cm^{-1} absorption peak is attributed to the tetrahedral structure of VO_4^{3-}, which indicates that the crystal structure of the sample is consistent with the tetragonal structure of YVO_4. The weak absorption peaks that appear in the range of 3300 cm^{-1} to 3500 cm^{-1} and 1350 cm^{-1} to 1700 cm^{-1} are attributed to O–H absorption. Moisture absorption by the samples mainly causes these peaks, which will disappear after heat treatment [19].

The hydroxyl ions are also assumed to enter the crystals from air during the growth process. The fact that the absorption band in the range of 3300 cm^{-1} to 3500 cm^{-1} belongs to OH^- has been proved using the method of isotopic substitution by Kovács et al. [20]. The weak absorption peak at 450 cm^{-1} could be attributed to Y–O absorption. The FTIR spectra of YVO_4 phosphor powder synthesized at other HRTs are basically similar to Fig. 4, with only a slight difference in intensity.

3.2. Optical properties

Absorption property, particularly in the region of ultraviolet and visible light, was tested using a spectrophotometer. The range of the test wavelength is 200 nm to 800 nm, and the results are shown in Fig. 5. The absorption edge of YVO_4 phosphor powders synthesized at different HRTs is almost 326 nm (i.e. band gap of approximately 3.8 eV), which is close to the wavelength limit of its intrinsic absorption transition. The effect of HRT on the absorption edge is not obvious. The ultraviolet absorption band is attributed to VO_4^{3-} absorption. However, differences are found for phosphor powder in the visible region absorption. The YVO_4 phosphor powder synthesized at 180 °C has better absorption properties in the visible region than the other YVO_4 phosphor powder materials synthesized at different HRTs.

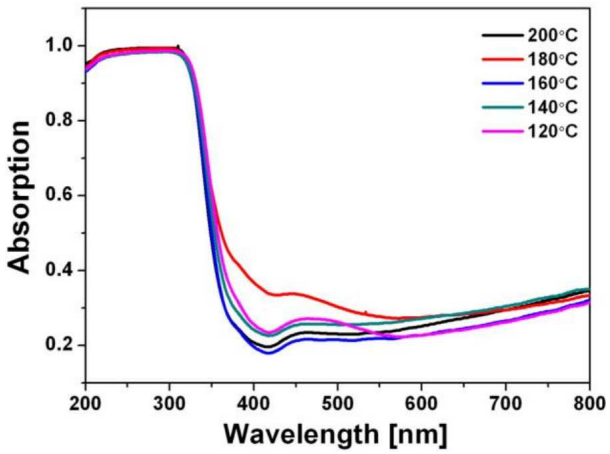

Fig. 5. Absorption spectra of the YVO_4 phosphor powders synthesized at different HRTs.

Figure 6 shows the photoluminescence spectra of the YVO_4 phosphor powders synthesized at different HRTs. A broad band emission extending from 350 nm to 650 nm is observed under the excitation of the 320 nm ultraviolet photon. The emission peaks are near 450 nm. The emission band observed in our experiment is in agreement with the emission of VO_4^{3-} reported in the literature [21].

The photoluminescence of pure YVO_4 are due to these transitions within the VO_4^{3-} ion since similar results are observed from "isolated" vanadate ions in similar hosts such as YPO_4 [22]. The VO_4^{3-} molecular ions have T_d symmetry and a vanadium–oxygen spacing of 1.72 Å.

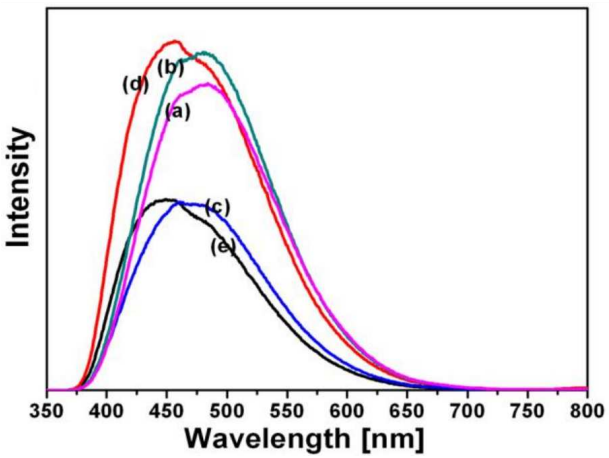

Fig. 6. Photoluminescence spectra of the YVO_4 phosphor powder synthesized at HRTs of (*a*) 120 °C, (*b*) 140 °C, (*c*) 160 °C, (*d*) 180 °C, (*e*) 200 °C.

When the vanadate ion is put into the YVO_4 crystal, its T_d symmetry is reduced to D_{2d} by the crystal field. This causes a splitting of some of the degenerate energy levels [23].

The photoluminescence observed in our experiment is attributed to the following steps. First, the VO_4^{3-} that absorbs an ultraviolet photon is excited from the filled oxygen $2p$ levels in the valence band to the empty V $3d$ levels of the conduction band. Second, the electrons in the excited state undergo Stokes shift and relax to the metastable state (i.e. the splitting levels) by the non-radiation transition of emitting different energy phonons. Finally, the excited electrons relax to the ground state by emitting a blue-green photon.

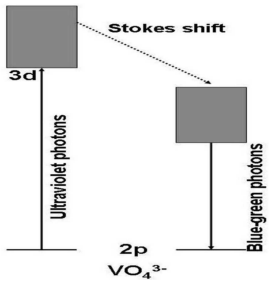

Fig. 7. The energy transfer diagram between ultraviolet photons and VO_4^{3-}.

Figure 7 shows the diagram of the energy transfer model. Pankratov et al. [24] reported an emission band near 3.1 eV in the intrinsic emission spectrum of YVO_4 crystal at a low temperature (80 K) in 2007. The intrinsic emission whose lifetime is shorter than that of the blue band emission is annihilated when the temperature is higher than 150 K [24]. This is consistent with the result of the non-intrinsic emission of the YVO_4 matrix materials in the PL spectra.

Figure 6 reveals that the YVO_4 phosphor powder synthesized at 180 °C exhibits the maximum photoluminescence intensity. This is associated with the lower defect density caused by the higher crystalline quality under 180 °C than the other HRTs in our experiment. The lower defect density directly leads to the decrease in non-radiative recombination. Thus, the photoluminescence intensity of radiative recombination shows the maximum value under 180 °C.

4. Conclusion

In this study, YVO_4 phosphor powders were synthesized using the hydrothermal method. The effect of HRT on the microstructure and the optical properties of the YVO_4 phosphor powders were analyzed, and the following conclusions were drawn:

(1) The macroscopic stress in the lattice of YVO_4 obviously changes with the elevated HRT. Moreover, a smaller average grain size results in a larger lattice microscopic distortion, which is due to the enhanced surface effect.

(2) The YVO_4 phosphor powder synthesized by hydrothermal method involves a certain agglomeration of small particles. The size of the particle is approximately in the micrometer scale. These phenomena are related to the randomness of crystal growth along each orientation during the hydrothermal process.

(3) The phonon vibration in the YVO_4 crystal lattice originates mainly from the internal vibrations in the vanadium–oxygen tetrahedron, in addition to the Y–O and O–H vibrations. Among the various kinds of common down-conversion matrix materials, YVO_4 crystal has low phonon energy of only 2.8188×10^{-21} J, which helps to improve the down-conversion efficiency of rare earth ions-doped YVO_4 phosphor powder.

(4) The band gap of approximately 3.8 eV for the YVO_4 synthesized in our experiment leads to good absorption properties in the ultraviolet region. Upon excitation by the 320 nm ultraviolet photon, the intrinsic emission of YVO_4 crystal is annihilated, and a broadband emission of VO_4^{3-} near 450 nm is observed at room temperature. The YVO_4 phosphor powder synthesized at 180 °C exhibits the maximum photoluminescence intensity, which is associated with the lower defect density caused by the higher crystalline quality under 180 °C.

Acknowledgments

We are grateful for the supports by the National Natural Science Foundation of China (grant No. 60807001), the Foundation of Young Key Teachers from University of Henan Province (grant No. 2011GGJS-008), the Foundation of Henan Educational Committee (grant No. 2010A140017) the Foundation of Graduate Innovation of Zhengzhou University (grant No. 12L00104) and the Foundation of Graduate Education Support of Zhengzhou University.

References

[1] A.K. Levine, F.C. Palilla, *Appl. Phys. Lett.* **5**, 118 (1964).

[2] H.J. Zhang, X.L. Meng, L. Zhu, P. Wang, X.S. Liu, Z.H. Yang, J. Dawes, P. Dekker, *Phys. Status Solidi A* **175**, 705 (1999).

[3] A.R. Forbes, C.D. McMillen, H.G. Giesber, J.W. Kolis, *J. Cryst. Growth* **310**, 4472 (2008).

[4] X.Y. Huang, Ph.D. Thesis, South China University of Technology, Guangzhou 2011 (in Chinese).

[5] P. Würfel, *Physica E* **14**, 18 (2002).

[6] L. Aarts, B. van der Ende, M.F. Reid, A. Meijerink, *Spectrosc. Lett.* **43**, 373 (2010).

[7] Z.H. Xu, X.J. Kang, C.X. Li, Z.Y. Hou, C.M. Zhang, D.M. Yang, G.G. Li, J. Lin, *Inorg. Chem.* **49**, 6706 (2010).

[8] X.Y. Huang, J.X. Wang, D.C. Yu, S. Ye, Q.Y. Zhang, X.W. Sun, *J. Appl. Phys.* **109**, 113526 (2011).

[9] H.Y. Xu, L. Jia, S.L. Xu, X.D. Li, H. Wang, H. Yan, *Acta Chim. Sinica* **63**, 612 (2005) (in Chinese).

[10] X.Y. Huang, D.C. Yu, Q.Y. Zhang, *J. Appl. Phys.* **106**, 113521 (2009).

[11] K.Y. Li, R.Z. Wang, M.H. Qu, Y. Zhang, H. Yan, *Chin. J. Lumin.* **33**, 486 (2012).

[12] X.Y. Huang, Q.Y. Zhang, *J. Appl. Phys.* **105**, 053521 (2009).

[13] X.C. Mi, Y.Y. Chen, Z.J. Wu, X.H. Liu, S.Y. Yang, L.C. Zhang, *PARTA: Phys. Test.* **40**, 181 (2004) (in Chinese).

[14] X.Y. Fan, S.M. Ma, *China Ceram. Indust.* **9**, 43 (2002) (in Chinese).

[15] X.Y. Gao, X.W. Liu, H.L. Feng, J.X. Lu, *J. Zhengzhou Univ. (Nat. Sci. Ed.)* **42**, 51 (2010) (in Chinese).

[16] B. Jin, S. Erdei, A.S. Bhalla, F.W. Ainger, *Mater. Lett.* **22**, 281 (1995).

[17] B.M. Jin, S. Erdei, A.S. Bhalla, F.W. Ainger, *Mater. Res. Bull.* **30**, 1293 (1995).

[18] J. Wang, Y.H. Xu, M. Hojamberdiev, J.H. Peng, G.Q. Zhu, *J. Non-Cryst. Solids* **355**, 903 (2009).

[19] M. Yu, J. Lin, Z. Wang, J. Fu, S. Wang, H.J. Zhang, Y.C. Han, *Chem. Mater.* **14**, 2224 (2002).

[20] L. Kovács, S. Erdei, R. Capelletti, *Solid State Commun.* **111**, 95 (1999).

[21] H. Ronde, G. Blasse, *J. Inorg. Nucl. Chem.* **40**, 215 (1978).

[22] G. Blasse, *Philips Res. Rept.* **24**, 131 (1969).

[23] C. Hsu, R.C. Powell, *J. Lumin.* **10**, 273 (1975).

[24] V. Pankratov, L. Grigorjeva, D. Millers, H.M. Yochum, *Phys. Status Solidi C* **4**, 801 (2007).